XIX International Conference on Water Resources
CMWR 2012
University of Illinois at Urbana-Champaign
June 17-22,2012

NUMERICAL MODELING OF FLOW THROUGH DOMAINS WITH SIMPLE VEGETATION-LIKE OBSTACLES

Steven A. Mattis[†], Clint N. Dawson[†], Christopher E. Kees[*] and Matthew W. Farthing[*]

[†] The University of Texas at Austin
The Institute for Computational Engineering and Sciences (ICES)
1 University Station C0200, Austin, Texas 78712

[*]U.S. Army Engineer Research and Development Center
Coastal and Hydraulics Laboratory, 3909 Halls Ferry Road,Vicksburg, MS 39180

Key words: Pore-scale modeling, vegetation, drag models

Summary. Using a variety of CFD and modeling techniques including large eddy simulation, we numerically calculate drag coefficients and qualitatively analyze drag characteristics for incompressible flows around simple, rigid, vegetation-like structures over a large range of Reynolds numbers. We compare our results to models for upscaling flow through porous media.

1 INTRODUCTION

Due to computational constraints, when modeling incompressible flow over and around porous structures or through heavily vegetated regions one must often use upscaling techniques to find parameterizations for resistance due to form drag. Using high resolution computational methods, we analyze these drag characteristics for flows ranging from those with very small Reynolds numbers to those that are turbulent through a variety of vegetated domains. This work is of importance to scientists and engineers dealing with wetland health and restoration, inland flooding due to tropical storms and hurricanes, and river lining projects. Flow resistance due to vegetation is a major factor in determining velocity and water level distribution in wetlands. The characteristics of this resistance depend greatly on the depth of the water, whether the vegetation is emergent or submerged, flexibility, foliage, and bottom roughness.

For low Reynolds numbers, wetlands behave similarly to porous media, where it is well-known that Stokes flow at the micro-scale can be upscaled through homogenization to Darcy's Law at the macro-scale. For higher Reynolds numbers, Stokes equation is no longer a valid approximation, and full Navier-Stokes models must be used. As Reynolds number increases moderately, small-scale drag effects can be captured by adding

extra terms to Darcy's Law giving various so-called "non-Darcy" models such as Darcy-Forchheimer. We analyze the accuracy of these models and over what range of Reynolds numbers for which they are valid. We utilize a variety of Large Eddy Simulation (LES) methods to study vegetative drag at high Reynolds numbers where turbulence is a significant concern. Our numerical simulations are performed using the Proteus Toolkit, which is under development by Kees and Farthing at ERDC. An expanded version of this work is presented by Mattis et al.[1]

2 THEORY

2.1 THE CONCEPT OF DRAG

Fluid viscosity causes resistance in the flow around immersed bodies. Viscous effects can produce three different types of resistance as described by Rouse[2]. At low Reynolds numbers, inertial effects of flow are negligible compared to those caused by viscous stress. We see that these viscous effects extend a great distance into the surrounding flow, causing a widespread distortion of the flow pattern. This is known as "deformation drag." At higher Reynolds numbers, the deformed region of the flow is much smaller, limited to a thin layer surrounding the body. Therefore the resulting shear is along the boundary surface. We call this "surface drag." If the form of the body is such that there is separation in the flow, it produces "form drag." In this scenario, there is a lower intensity of pressure in the wake of the object which causes a resultant force which opposes the motion. Under certain conditions form drag can reduce viscous stresses to insignificant values.

We write the relationship for the force of drag opposing motion as

$$F = C_d A \frac{\rho V^2}{2} \tag{1}$$

where F is the drag force, A is the cross sectional area of the body, V is the magnitude of the velocity of the flow, and C_d is a drag coefficient. We note that C_d is dependent on Reynolds number. In multiple dimensions, we can write the drag equation as $\mathbf{F} = \mathbf{C_d} A \frac{\rho |\mathbf{V}| \mathbf{V}}{2}$ where now $\mathbf{C_d}$ is a tensor and $\mathbf{V}$ is the mean velocity vector. For calculating $\mathbf{C_d}$, we take $\mathbf{F}$ as the hydraulic gradient $\mathbf{F} = -LA(\nabla p - \rho \mathbf{f})$ where L is the domain length and $\mathbf{f}$ is a forcing term which includes the gravitational constant.

2.2 LOW REYNOLDS NUMBER FLOWS

We will use some techniques from the study of flow through porous media for our analysis of flow through vegetated regions. Tightly packed vegetation can be analogous to a porous medium. We define Reynolds number as $Re = \frac{Vd}{\nu}$ where V is the mean flow rate over the total volume including the obstructions (specific discharge), d is the mean diameter of the individual plants, and ν is the kinematic viscosity of the fluid. Viscous forces dominate, so inertial effects can be ignored. For very low Reynolds number flows

($Re < 1$) Darcy's Law,

$$\mathbf{V} = -\frac{-\mathbf{K}}{\mu}(\nabla p - \rho \mathbf{f}), \tag{2}$$

where $\mathbf{V}$ is the mean velocity vector, ∇p is the pressure gradient, $\mathbf{K}$ is the "hydraulic permeability" tensor with units L^2, μ is the dynamic viscosity of the fluid, ρ is the fluid density, and $\mathbf{f}$ is the forcing vector containing the gravitational constant, is the basic constitutive equation for flow in porous media. The hydraulic permeability tensor depends solely on the properties of the porous medium. The flow is divergence free:

$$\nabla \cdot \mathbf{V} = 0. \tag{3}$$

Darcy's Law is mathematical derived by homogenization of the Stokes equations. See Hornung[3] for the calculation of $\mathbf{K}$ and derivation.

2.3 HIGHER REYNOLDS NUMBER FLOWS

For flows with Reynolds numbers greater than 1 the inertial forces become much greater than the viscous forces and dominate. The inertial terms in Navier-Stokes are no longer negligible, so the homogenization of Stokes equation is no longer the correct upscaling. Forchheimer noticed from empirical results that for higher Reynolds numbers, the relationship resembles Darcy's Law plus a quadratic term. This is called the Darcy-Forchheimer equation[4]:

$$-(\nabla p - \rho \mathbf{f}) = \mu \mathbf{K^{-1}} \mathbf{V} + \beta \rho |\mathbf{V}| \mathbf{V}. \tag{4}$$

It has been observed to be accurate for moderate Re experimentally[5] and computationally[6]. There have been many attempts at deriving the Darcy-Forchheimer Law using mathematical homogenization[7], but the results of these studies sees

$$-(\nabla p - \rho \mathbf{f}) = \mu \mathbf{K^{-1}} \mathbf{V} + \beta \rho |\mathbf{V}|^2 \mathbf{V}. \tag{5}$$

This has been verified numerically for very small Reynolds numbers; however, this has only been verified where Darcy's Law is approximately valid, and the quadratic law seems to be more appropriate for higher Reynolds number flows. Some[8], have also used power laws of the form,

$$-(\nabla p - \rho \mathbf{f}) = \mu \mathbf{K^{-1}} \mathbf{V} + \alpha_1 \mathbf{V}^{\alpha_2} \tag{6}$$

to fit empirical data. For (5) and (6), β, α_1, and α_2 are model parameters that must be found empirically.

From experimental data we know that as Reynolds number increases above the region where Darcy's Law is valid, the nature of the flow changes. At low Reynolds numbers we see deformation drag; streamlines are greatly affected by the obstacles. As Reynolds number increases, we see separation occur and form drag occurs with less deformation. Eventually, streamlines shift and fixed eddies form in the wake of obstacles. The size of the eddies increases as Re increases. Around $Re = 70$ turbulence begins to occur. When

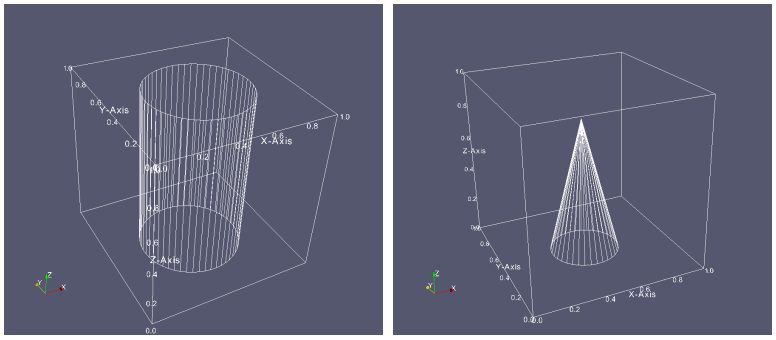

Figure 1: Emergent cone domain (left) and submerged cone domain (right).

Re reaches 75 the flow is turbulent in approximately half of the domain, and when Re nears 200 there is turbulence everywhere in the flow[5]. At high Reynolds numbers we see the drag force begin to balance with the driving force. Therefore, we see C_d become constant. In subsurface modeling, it is uncommon to deal with Reynolds numbers this large, so we must use other techniques.

2.4 NAVIER-STOKES AND LARGE EDDY SIMULATION

To study drag at higher Reynolds number flows where nonlinear behavior occurs, we need to analyze the full Navier-Stokes equations. In order to capture the large-scale effects of turbulence without the need to resolve smaller turbulence length scales, we use Large Eddy Simulation with the Smagorinsky filter. The Smagorinsky LES filter models an eddy viscosity ν_T by $\nu_T(\mathbf{x}) = (C_s\Delta_g)^2\sqrt{2\overline{S_{ij}}\,\overline{S_{ij}}}$, where the filter size Δ_g (m) is set to the grid size, C_s is the Smagorinsky constant, and $\overline{S_{ij}} = \frac{1}{2}\left(\frac{\partial \overline{v_i}}{\partial x_j} + \frac{\partial \overline{v_j}}{\partial x_i}\right)$ is an entry of the filtered strain rate tensor, providing closure for the filtered Navier-Stokes Equations

$$\nabla \cdot \overline{\mathbf{v}} = 0 \tag{7}$$

$$\frac{\partial \overline{\mathbf{v}}}{\partial t} + \nabla \cdot (\overline{\mathbf{v}} \otimes \overline{\mathbf{v}} - (\nu + \nu_T)\nabla \overline{\mathbf{v}}) + \frac{\nabla \overline{p}}{\rho} - \overline{\mathbf{f}} = 0. \tag{8}$$

The standard Smagorinsky model takes C_s as a constant, generally between 0.1 and 0.3; however, this assumes homogeneous isotropic turbulence and filter scale in the inertial subrange. We deal with this type of turbulence as well as lamniar flow, transitional flow, and sheared flows that do not have that structure. Germano et al.[9] developed a model for calculating C_s dynamically in each region of the flow. There are more practical methods[10] for calculating C_s. By assuming a Pao turbulent energy spectrum, for fully laminar flows we take $C_s = 0$, and for transitional and turbulent flows, we take

$$C_s^2(Re_\Delta) = 0.027 \times 10^{-3.23 Re_\Delta^{-0.92}} \tag{9}$$

where $Re_\Delta = \frac{\Delta_g^2 \sqrt{2\overline{S_{ij}}\,\overline{S_{ij}}}}{\nu}$ is the mesh-Reynolds number at a given point in the flow.

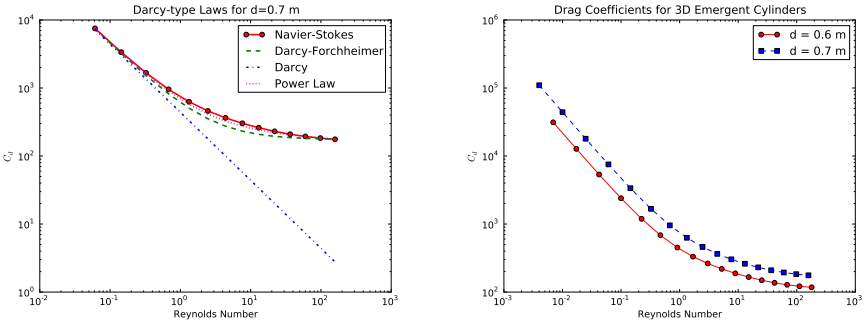

Figure 2: A comparison of C_d calculated from Darcy and non-Darcy laws for flow around an emergent cylinder with d=0.7m (left) and C_d calculated with LES simulations over a large range of Re for emergent cylinders with different diameters (right).

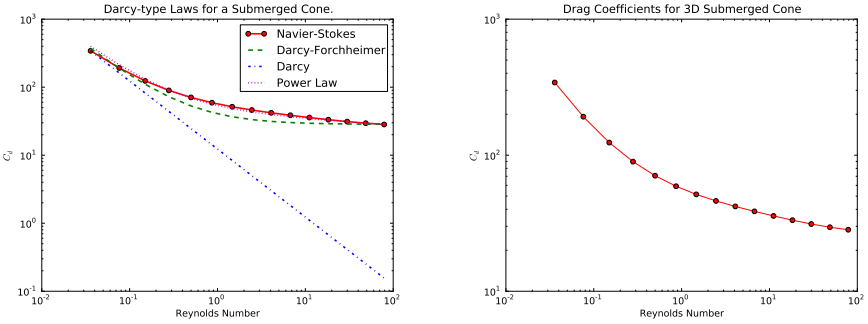

Figure 3: A comparison of C_d calculated from Darcy and non-Darcy laws for flow around a submerged cone with a base radius of 0.25 m and a height of 0.8 m (left) and C_d calculated with LES simulations over a large range of Re for the submerged cone (right).

3 NUMERICAL METHOD

We use a locally conservative, stabilized finite element method[11] to find weak solutions to (8) with given forcing functions $\mathbf{f}$ given zero initial conditions, periodic boundary conditions on the sides, a free surface condition on the top, and a no-slip condition on the bottom and obstacles. In some cases, while solving (8) we ignore the time derivative and solve for a steady-state solution. For higher Re cases we use implicit time stepping until the mean velocities reach a stationary state. We utilize linear Lagrangian basis functions

on unstructured tetrahedral meshes. We calculate C_d from $\mathbf{f}$ and the resulting volume averaged velocity $\mathbf{V}$. All simulations were run in parallel on Texas Advanced Computing Center (TACC) machines.

4 RESULTS

4.1 3D EMERGENT CYLINDER EXAMPLE

The three-dimensionality of vegetation has a major effect on flow behavior. Flow behaves differently depending on whether or not the vegetation is completely submerged or whether it rises above the fluid level. If it is completely submerged, then the flow height is important. The bed also has a major effect on the flow.

We consider a cubic domain with a cylindrical obstacle as seen in Figure 1. Figure 4 shows velocity magnitude and streamlines for a flow with $Re = 60.15$. We observe surface drag in this figure.

We calculate $\mathbf{K}$ using mathematical homogenization and perform parameter fitting to estimate parameters for non-Darcy laws. We use data from the full range of Reynolds numbers to fit for the parameters necessary for the non-Darcy laws. The resulting drag coefficients or flow around a cylinder of diameterr 0.7 m using the upscaling techniques are shown in Figure 2. C_d over a large range of Re for different diameter cylinders are also shown in Figure 2. Darcy's Law is valid for very small Re (< 1). The Darcy-Forchheimer equation and the power law match the Navier-Stokes data quite well over the whole range of Re.

4.2 3D SUBMERGED CONE PROBLEM

This simulation is most like a real world flow over submerged vegetation. The problem uses the submerged cone domain in Figure 1. It models the behavior of flow through a periodic bed of completely submerged plants. The 3D behavior of this flow is much more complex than that in the previous example. There are nontrivial vertical velocities in sections of the domain. By driving flow with range of hydraulic gradients $\mathbf{F}$ to steady-state we see the flow structure and upscaled results for a variety of Reynolds numbers. The cones in these simulations have a height of 0.8 m and base radius of 0.25 m and are located in the center of the cell. For our scaling parameter d we use 0.35 m, the diameter at the center of mass.

Figure 5 shows results from a low Reynolds number flow with $Re = 6.3$. Notice the 3D behavior in the streamlines. There is vast flow deformation in the horizontal and vertical directions around and over the cone. In the vertical slice, we see a thin boundary layer around the bottom and the cone with standard logarithmic velocity profile. This displays the effects of form drag in the vertical direction.

As with the previous example, we look at Darcy and non-Darcy upscaling results. In Figure 3 we see similar results to the 3D cylinder problem. At low Re Darcy's Law and Darcy-Forchheimer match very well with Navier-Stokes data. At higher Re, Darcy's Law

become completely invalid and Darcy-Forchheimer and a power law provide reasonable approximations for C_d. The full range of simulations were used to fit for the various non-Darcy model parameters.

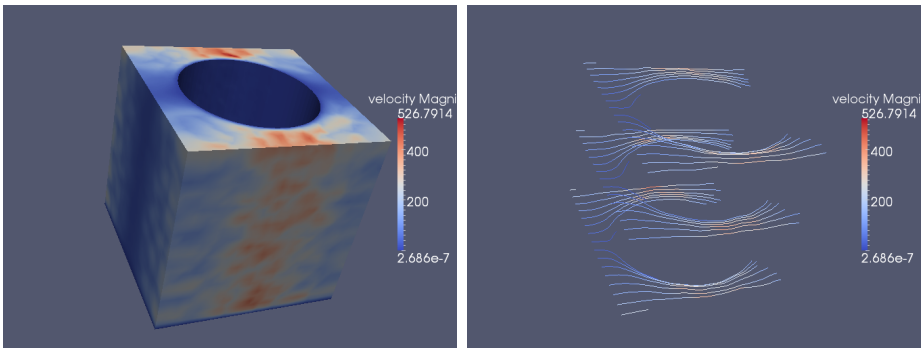

Figure 4: Velocity magnitude (left) and streamlines (right) for flow around an emergent cylinder of diameter 0.7 m at $Re = 60.15$.

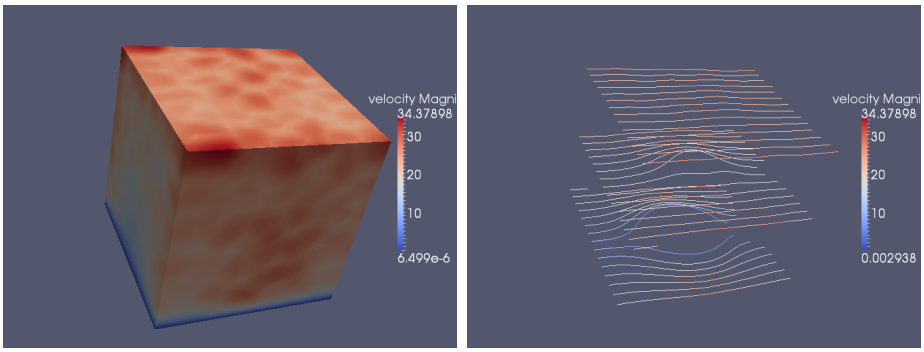

Figure 5: Velocity magnitude (left) and streamlines (right) for flow around a submerged cone of base diameter of 0.5 m and a height of 0.8 m at $Re = 6.3$.

5 CONCLUSIONS

Flow through porous structures and vegetated domains can be quite complex. For very low Re flows Darcy's Law accurately and effectively models the mean flow. Using mathematical homogenization, the resulting hydraulic conductivities can be relatively easily calculated. However, for higher Re flow, it is not as simple. Non-Darcy models such as Darcy-Forchheimer provide more accurate results than Darcy's Law; however, they require important parameters to be estimated and are not effective over large ranges of

Re. The most descriptive way of displaying the drag effects on these types of domains over a large range of *Re* is a chart similar to a Moody diagram. Creating this would require performing extensive computational simulations over many different packings of vegetation and many Reynolds numbers. This approach might allow for a semi-automated system for taking remotely sensed geometry information (i.e. using LiDAR) and calculating parametrized resistance factors. Further work remains for issues such as depth dependance with submerged vegetation, flexible stems, foliage, and potential issues like wave/current/vegetation interaction.

REFERENCES

[1] S.A. Mattis, C.N. Dawson, C.E. Kees and M.W. Farthing. Numerical modeling of drag for flow through vegetated domains and porous structures. *Advances in Water Resources.* **39**, 44-59, (2012).

[2] Hunter Rouse. *Fluid mechanics for hydraulic engineers*, McGraw-Hill, (1938).

[3] Ulrich Hornung. Homogenization and porous media. *Inerdicip. Appl. Math.* Vol. 6, Springer, (1997).

[4] P. Forchheimer. Wasserbewegung durch Boden. *Zeit. Ver. Deut. Ing.* **45**, 1781-1788, (1901).

[5] Jacob Bear. *Dynamics of fluids in porous media.* Dover, (1988).

[6] C. Garibotti and M. Peszyńska. Upscaling non-Darcy flow. *Transport in porous media.* **80**(3). 401-430. (2009).

[7] M. Balhoff, A. Mikelić, and M.F. Wheeler. Polynomial filtration laws for low Reynolds number flows through porous media. *Transport in Porous Media.* **8**, 35-60, (2010).

[8] A.E. Scheidegger. *The physics of flow through porous media.* Revised edition. The Macmillan Co,. New York, (1960).

[9] M. Germano, U. Piomelli, P. Moin and W. Cabot. A dynamic subgrid-scale eddy viscosity model. *Phys Fluids A: Fluid Dynam.* **3**. 1760. (1991)

[10] P. Voke. Subgrid-scale modelling at low mesh reynolds number. *Theort Comput Fluid Dynam.* **8**(2). 131-143. (1996).

[11] C.E. Kees, M.W. Farthing and M.T. Fong. Locally conservative, stabilized finite element methods for a class of variable coefficient Navier-Stokes equations, U.S. Army Engineer Research and Development Center, Coastal and Hydraulics Laboratory, TR-09-12, (2009).